

X-Ray Photoemission from Zinc: Evidence for Extra-Atomic Relaxation via Semilocalized Excitons*

L. Ley, S. P. Kowalczyk, F. R. McFeely, R. A. Pollak,[†] and D. A. Shirley

Department of Chemistry and Lawrence Berkeley Laboratory, University of California, Berkeley, California 94720

(Received 12 March 1973)

X-ray-photoelectron-spectroscopy studies on clean metallic zinc are reported. A well-defined Fermi edge was observed, and the $3d$ -band peak was located at $E_F - 10.2$ eV. The data analysis raised the question of the extent to which valence-band photoemission spectra of metals are distorted, relative to one-electron "frozen-orbital" band-structure calculations, by differential relaxation. Atomic hole-state calculations by Lindgren and by Gelius and Siegbahn indicate that (intra-) atomic relaxation can vary by up to 5 eV between $3d$ and $4s$ shells. Thus valence-band spectra in $3d$ transition metals can be seriously distorted by atomic relaxation alone. It is argued that the $3d$ bands probably lie below the $4s, 4p$ valence bands in zinc in the *initial* state, but not in the photoemission spectrum. The nickel photoemission spectrum may well be distorted by relaxation. The magnitude of the extra-atomic relaxation energy ΔE_B was estimated in several ways. Empirical estimates were based on comparisons among photoemission and optical data on several elements. Semiempirical estimates were based on theoretical atomic binding energies and experimental binding energies in metals. All estimates were in rather good agreement, showing extra-atomic relaxation energies of up to ~ 15 eV. A theoretical model was derived, based on the assumption that extra-atomic relaxation occurs through screening of the hole state by formation of a semilocalized exciton. This process was described by Friedel as positive phase shifts in the conduction bands. The model predicts a slow rise in ΔE_B in the $3d$ series and a sudden drop between Ni and Cu, in excellent agreement with experiment.

I. INTRODUCTION

Zinc is of particular interest as a prototypical metal for high-energy valence-band studies. With a free-atom ground-state configuration $3d^{10} 4s^2$, zinc as a metal is expected to exhibit a density of states that can be cleanly resolved into a narrow, high, $3d$ -band peak and a low, wide, $4s, 4p$ band. The $3d$ band should lie far enough below the Fermi energy E_F to be nearly corelike, while E_F should fall in the $4s, 4p$ band. Indeed, this general behavior was established in several earlier experimental¹⁻⁵ and theoretical⁶⁻⁹ studies.

In this paper we report an x-ray-photoelectron-spectroscopy (XPS) study on metallic zinc. The Fermi edge was observed very clearly, in contrast to earlier "high-energy" studies. The $3d$ -band peak position was located directly relative to E_F , at $E_F - 10.2$ eV in the spectrum. This last qualification—"in the spectrum"—appears to be very important, because the analysis presented below suggests that the $3d$ binding energy is lowered considerably by relaxation relative to its value as estimated from ground-state band-structure calculations, using the frozen-orbital (Koopmans's-theorem) approximation. Thus after zinc is dealt with in Secs. II and III, the discussion is broadened to deal with the phenomenon of atomic relaxation, in Sec. IV. Evidence for extra-atomic relaxation is reviewed in Sec. V. A theoretical model for describing extra-atomic relaxation in terms of screening is developed in Sec.

VI, and predictions of relaxation energies are made and compared to experiment. Conclusions are drawn in Sec. VII.

II. EXPERIMENTAL

A high-purity single crystal of zinc was irradiated with monochromatized $AlK\alpha_{1,2}$ x rays in a Hewlett-Packard 5950A ESCA Spectrometer that had been modified to operate at pressures $\leq 10^{-9}$ Torr after baking. Immediately before the photoemission experiments the sample was argon-ion bombarded for 6 min, using an argon pressure of 7×10^{-5} Torr and an accelerating voltage of 1000 V. Before ion bombardment a prominent oxygen-1s peak was present. It showed a doublet structure, presumably due to adsorbed oxygen-containing molecules (at $E_F - 532.8 \pm 0.3$ eV) and oxygen bonded to zinc (at $E_F - 531.3 \pm 0.3$ eV). The 532.8-eV line went away first on ion bombardment, followed by the 531.3-eV line, which showed a final intensity a factor of 40 smaller than the total O-1s intensity before ion bombardment. After 19 h, when the photoemission runs were finished, the oxygen-1s intensity had increased by not more than a factor of 2. The oxygen-2p peak usually falls about 10 eV below E_F . In this case we estimate that the O-2p peak would be under the Zn-3d peak, with an intensity ratio $I(\text{Zn } 3d)/I(\text{O } 2p) \cong 50$. We estimate the oxygen impurity content as equivalent to $\sim \frac{1}{3}$ monolayer on the average.

The valence band was studied, as were the $2s$, $2p$, $3s$, and $3p$ lines. Every spectrum was run

at least twice, and the results were in excellent agreement in each case.

III. RESULTS

Figures 1-3 show, respectively, spectra of the $2s$, $2p_{1/2}$, $2p_{3/2}$ region, of the $3s$, $3p_{1/2}$, $3p_{3/2}$ region, and of the $3d$ - $4s$, $4p$ valence bands. Derived binding energies relative to E_F are set out in Table I.

In the $n=2$ shell the three lines are well separated (Fig. 1). The $2s$ line is relatively wide, and its Lorentzian shape suggests lifetime broadening. The $2p$ lines are much narrower but still considerably wider, 2-eV full width at half-maximum (FWHM), than the instrumental resolution ~ 0.5 eV. Their width probably arises mainly from lifetime broadening (note particularly the Lorentzian-like "tail" on the low- E_B side of the $2p_{3/2}$ line in Fig. 1) and from final-state effects, which produce a marked asymmetry in both $2p$ lines.

Direct comparison of the $2s$ and $2p$ binding energies with theory is not possible. No theoretical values for core hole-state energies in zinc are available, and it is probably not feasible to calculate such energies directly at this time. However, it is possible to estimate atomic binding energies for these states by using published calculations on copper and zinc and a somewhat involved argument. These energies are estimated in this way below and compared with our experimental values because of the relevance of this comparison to

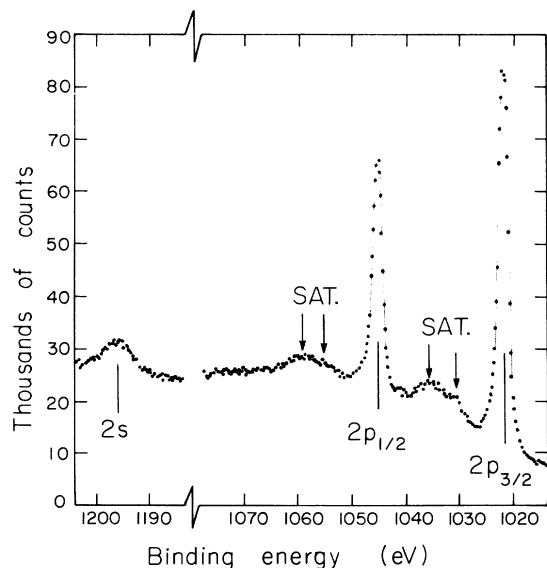


FIG. 1. XPS spectrum of the $n=2$ peaks of zinc. Alternate points are omitted for clarity except in the $2p$ peaks. Satellite structure is indicated by arrows at 9 and ~ 14 eV below each $2p$ peak.

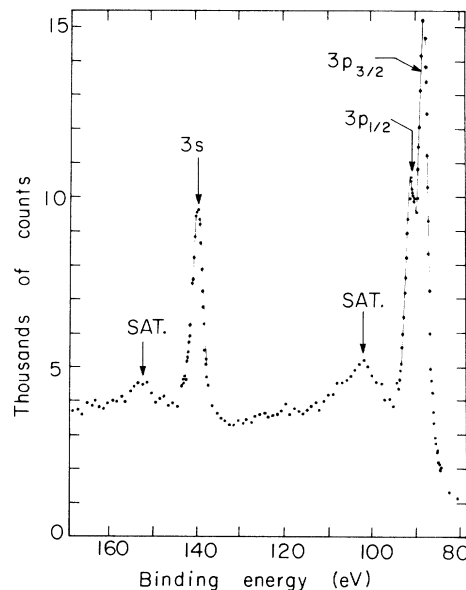


FIG. 2. XPS spectrum of the $3s$, $3p$ peaks of zinc. Except in peaks themselves, only every fifth point is shown.

the discussion of extra-atomic relaxation in Secs. V and VI.

J. B. Mann¹⁰ has given nonrelativistic Hartree-Fock orbital energies ϵ_{nr} for the elements. Rosén and Lindgren¹¹ gave relativistic optimized Hartree-Fock-Slater orbital energies ϵ_r and binding energies E_B for core levels in atomic copper. To estimate core-level binding energies in atomic

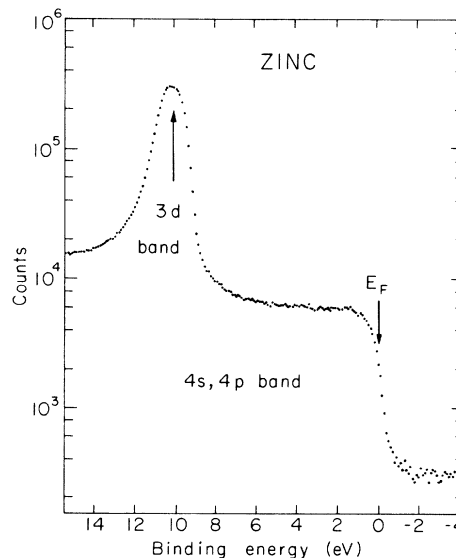


FIG. 3. XPS valence-band spectrum of zinc, on a semilogarithmic scale.

TABLE I. Experimental energies (in eV).

Feature	E_B^F	FWHM	Rel. intensity ^a
2s peak	1196.16(25)	5.5(5)	0.19
2p _{1/2} peak	1045.09(15)	1.95(5)	0.58
2p _{3/2} peak	1021.96(15)	2.00(5)	1
2p satellites	~ 9 and 14 eV below each 2p peak	2 broad peaks, 8–10-eV total width	0.30(5) relative to each 2p
2p _{1/2} -2p _{3/2} splitting	23.15(5)
3s peak	139.88(15)	2.62(10)	0.035
3p _{1/2} peak	91.31(15)	2.6(2)	0.039
3p _{3/2} peak	88.70(15)	2.6(2)	0.067
3p splitting	2.60(2)
3d peak	10.18(10)	1.45(2)	0.042
4s, 4p bands	0 to ≥ 10	≥ 10	0.006

^aThese ratios are accurate to about ± 10%.

zinc, we use the recipe

$$E_B(nl, Zn) \cong -\epsilon_{nr}(nl, Zn)\epsilon_r(nl, Cu)/\epsilon_{nr}(nl, Cu) + [E_B(nl, Cu) + \epsilon(nl, Cu)].$$

Here the second term is an atomic relaxation energy. The usual sign convention, in which for bound states $\epsilon < 0$ but $E_B > 0$, is used here.

Weighted average energies for np states were used throughout, because ϵ_{nr} does not include spin-orbit splitting. Zinc core-level atomic binding energies estimated in this way are given in Table II, together with corresponding values of $E_B^V = E_B^F + \phi_{Zn}$, the vacuum-level referenced metallic zinc binding energies obtained by adding the work function ϕ_{Zn} to the experimental binding energies. The experimental (metal) binding energies are lower by 3–8 V than the estimated atomic values.

The 2p_{1/2}-2p_{3/2} spin-orbit splitting of 23.15 ± 0.05 eV is slightly smaller than the value 24.8 eV obtained by taking the difference between free-atom Hartree-Fock-Slater (HFS) energy eigenvalues.¹²

Satellite or loss structure is associated with every core-level peak. For the broad (and weak) 2s peak no details are resolved, losses appearing as a higher background on the low-kinetic-energy (high- E_B) side. The other lines all show distinct satellites, peaking at ~ 12–13 eV below the main line. The satellites associated with the 2p lines are the best characterized in this work, because of the high intensities and narrowness of these lines. Particularly for the 2p_{3/2} line, the broad satellite peak may be resolved into two or more components, at ~ 9 and 14 eV. We have not studied

the satellite structure intensively, and it appears unlikely that a single, unique interpretation of this structure can be made on the basis of our data. It is not even clear to what extent the satellite structure is intrinsic and to what extent extrinsic to the localized hole state. Since the satellites appear to differ in form from one core line to another, they are probably at least partially intrinsic.

Most of the above comments about the $n = 2$ peaks apply also to the 3s and 3p_{1/2}, 3p_{3/2} peaks. Experimental and estimated theoretical binding energies for these orbitals are also set out in Table II. The 3p spin-orbit splitting of 2.60

TABLE II. Core-level binding energies in zinc (eV).

Level	$E_B(\text{atomic})^a$	$E_B^V{}^b$	$\Delta E_B{}^c$
2s	1205.3	1199.9	5.4
2p ^d	1036.3	1033.4	2.9
3s	149.4	143.6	5.8
3p ^d	97.9	93.3	4.6
3d ^d	15.3	13.9	1.4
	16.1 ^e		2.2

^aEstimated from results in Refs. 10 and 11 by method given in text.

^bExperimental binding energy referred to vacuum level, using $\phi(Zn) = 3.7$ eV.

^c $\Delta E_B = E_B(\text{atomic}) - E_B^V$.

^dMean values without spin-orbit splitting.

^eObtained by using Mann's orbital energy plus the relaxation correction of Ref. 11 for Cu.

± 0.02 eV is also somewhat lower than the HFS value¹² of 3.20 eV. In both the $n=2$ and $n=3$ shells the $(p_{1/2})/(p_{3/2})$ intensity ratio is 0.58 rather than the multiplicity ratio of $\frac{1}{2}$.

Moving up to the valence-band spectrum (Fig. 3), we find a $3d$ band peak centered at 10.18 ± 0.10 eV below E_F . The $4s, 4p$ band is low and flat, and the Fermi edge is clearly visible, with a (signal)/(background) ratio of > 50 . Since the $(3d)/(4s, 4p)$ height ratio is also 50, the spectrum is conveniently plotted on a semilogarithmic scale. Unfortunately none of the published theoretical band-structure calculations on zinc⁶⁻⁹ were accompanied by density-of-states plots, so it is not clear whether the calculated $4s, 4p$ bands would be in more than qualitative agreement with Fig. 3. The previous experimental studies of zinc¹⁻⁵ give results in only fair agreement among themselves. The ultraviolet-photoelectron-spectroscopy (UPS) studies^{3,5} and the newer soft-x-ray work⁴ appear to have given very precise results on well-characterized materials. In the soft-x-ray work the actual binding energy could not be determined directly, but the $3d-2p_{3/2}$ transition gave a peak energy of 1011.6 eV. Combining this with our $E_B^F(2p_{3/2}) = 1021.96 \pm 0.15$ eV from Table I, we deduce $E_B^F(3d) = 10.36 \pm 0.15$ eV, in reasonably good agreement with our XPS result. The UPS values of 9.5³ and 9.46⁵ are substantially lower, and the discrepancy appears to lie well outside of any reasonable estimates of experimental error. Further study will be needed to resolve this discrepancy. In the course of trying to explain it in terms of partial relaxation around a $3d$ -hole state, we have examined carefully the available data on atomic and extra-atomic relaxation in conductors. The results of this work are discussed in Secs. IV-VII.

IV. ATOMIC RELAXATION

To establish a basis for the discussion of extra-atomic relaxation toward a hole state in Sec. V, it is first necessary to consider atomic relaxation. That photoemission from deep-lying core states can be accompanied by complete relaxation is generally accepted, and core-level binding energies that include relaxation can be obtained by direct calculations of hole-state energies.¹⁰ Recently a simple model¹³ was used to estimate relaxation energies of deep core hole states due to "outer-shell" relaxation, giving excellent agreement with experiment for rare gases. In this work, however, we are interested in the relaxation energies of orbitals like the $3d$ shell in zinc, which form closed shells but are not deep core states. Since these relaxation energies are small and we wish to obtain accurate values, we must examine the experimental evidence carefully.

First let us recall the meanings of the various energy parameters. The orbital energy ϵ from a Hartree-Fock calculation gives, by Koopmans's theorem,¹⁴ (minus) the value of the binding energy E_B which that orbital *would* have if there were no relaxation. The actual binding energy can be obtained theoretically either by reducing the orbital energy in magnitude by a calculated relaxation energy E_R ,

$$E_B = -\epsilon - E_R, \quad (1)$$

or from direct calculation of the total energies of the initial and final states,

$$E_B = E_f - E_i. \quad (2)$$

Hartree-Fock-Slater (HFS) calculations give one-electron eigenvalues that are neither true orbital energies nor binding energies. Thus Koopmans's theorem does not apply to HFS eigenvalues.¹¹ However, *optimized* HFS give eigenvalues that are essentially identical to Hartree-Fock orbital energies as well as total energies essentially identical to Hartree-Fock total energies.¹¹ Thus, optimized HFS theory can be used to give binding energies via either of the above relations. Of course these theoretical estimates of E_B are still subject to the limitations of Hartree-Fock theory. Thus no allowance is made for electron correlation. There are, however, optical data available that establish the atomic binding energies of electrons in near-core levels for several elements. In Table III are listed the experimental binding energies taken from tabulated data,¹⁵ the orbital energies,^{10,11} and binding energies from total energy differences,^{11,16} for both the outermost s orbital and the next most loosely bound (p or d) orbital for the five elements of configuration p^6s , $d^{10}s$, or $d^{10}s^2$ for which we have been able to find the necessary data.

It is clear from Table III that the orbital energies ϵ are well in hand, with the two calculations^{10,11,16} showing good agreement in most cases. The relaxation energies are perhaps less well understood, with the theoretical values being somewhat too high in most cases. Of course the "experimental" rearrangement energy $\Delta E_B(\text{expt})$ includes correlation effects, while the theoretical relaxation energy $\Delta E_B(\text{theo})$ does not. Two features of Table III are of special relevance to the zinc photoemission problem. First, the rearrangement energies of near-core filled-shell states (p in p^6s , d in $d^{10}s$ or $d^{10}s^2$) are positive (i. e., $E_B < |\epsilon|$), and typically ~ 3 eV for d shells, while for the outer s orbitals in these configurations they are small or even negative. Second, there is available from optical data a binding energy for the $3d$ orbital in atomic zinc.

TABLE III. Atomic binding energies and rearrangement energies (in eV).

Ground-state configuration	Active orbital	$-\epsilon(\text{HF})^a$	$-\epsilon(\text{OHFS})^b$	$\Delta E(\text{theo})^b$	$E_B(\text{HF})^c$	$E_B(\text{OHFS})^b$	$E_B(\text{expt})^d$	$\Delta E(\text{expt})^e$
Na($2p^6 3s$)	$2p$	41.31	41.0	4.4	36.9	36.6	38.05	3.26, 2.95
K($3p^6 4s$)	$3p$	25.97	25.9	24.57	1.40, 1.3
Cu($3d^{10} 4s$)	$3d$	13.22	12.43	5.26	7.96	7.17	10.44	2.78, 1.99
Zn($3d^{10} 4s^2$)	$3d$	21.29	...	(5.26) ^f	(16.03)	...	17.31	3.98
Cd($4d^{10} 5s^2$)	$4d, ^2D_{3/2}$	(21.06) ^g	18.28	(2.78)
Cd($4d^{10} 5s^2$)	$4d, ^2D_{5/2}$	(20.36) ^g	17.58	(2.78)
Na($2p^6 3s$)	$3s$	4.95	5.0	-0.3	5.25	5.3	5.14	0.19, 0.14
K($3p^6 4s$)	$4s$	4.01	4.1	4.34	-0.33, -0.24
Cu($3d^{10} 4s$)	$4s$	6.49	6.86	0.28	6.21	6.58	7.72	-1.23, -0.86
Zn($3d^{10} 4s^2$)	$4s$	7.96	9.39	-1.43
Cd($4d^{10} 5s^2$)	$5s$	7.21	8.99	-1.78

^aFrom Ref. 10.^bFrom Refs. 11 and 16.^c $E_B(\text{HF}) = -\epsilon(\text{HF}) - \Delta E(\text{theo})$.^dFrom Ref. 15. Except for Cd, mean multiplet

energies are given.

^e $\Delta E(\text{expt}) = -\epsilon - E_B(\text{expt})$.^fValue for Cu.^gUsing a spin-orbit splitting of 0.70 eV.

V. EXTRA-ATOMIC RELATION

In this section we examine in several subsections the evidence that binding energies of atomic core and quasicore levels are different in conductors than in free atoms. As shown below, the available data clearly establish that

$$\Delta E_B = E_B(\text{atom}) - E_B(\text{conductor}) \quad (3)$$

is always positive, as indicated earlier.¹³ At the end of the section arguments are presented for interpreting ΔE_B as arising in large part from extra-atomic relaxation.

A. X-Ray Photoemission and Optical Data

The Zn($3d$) binding energy from this XPS work (Tables I and II) and the atomic binding energy from optical data (Table III) can be compared directly. Similar comparisons can be made for Cu($3d$)¹⁷ and for Cd($4d$).¹⁸ All three are summarized in Table IV. Recently the $4f_{7/2}$ binding energies in Pb and Bi have been measured.¹⁹ These are also included in Table IV, together with our values for $E_B^F(4f_{7/2})$, for the metals. The metal binding energies are referred to the vacuum level by adding the work function to the binding energy referred to the Fermi level,

$$E_B^V = E_B^F + \phi. \quad (4)$$

Work functions²⁰ of 3.7 eV (Zn), 4.5 eV (Cu), 3.9 eV (Cd), 4.05 eV (Pb), and 4.3 eV (Bi) were used.

It is evident from Table IV that the d orbitals in these metals have ΔE_B values of about 3 eV.

B. X-Ray Photoemission and Theoretical Atomic Core-Level Binding Energies

For deeper core levels optical data are no longer available. It is still possible in a few cases to compare measured core-level binding energies in the solid elements with theoretical atomic core-level binding energies. In the course of other XPS studies on the elements we have obtained core-level binding energies for orbitals in carbon (as graphite), aluminum, and copper. In Table V these are compared with theoretical binding energies for the atoms, from published optimized HFS calculations.¹⁶

Additional comparisons are available from the work of Siegbahn *et al.*¹⁶ They gave experimental

TABLE IV. Comparisons of E_B^V and $E_B(\text{atomic})$ in gases and metals (in eV).

Level	E_B^F	ϕ^a	E_B^V	$E_B(\text{atomic})$	ΔE_B
Cu($3d$)	3.0(1) ^b	4.5	7.5	10.44 ^c	2.9
Zn($3d$)	10.18(15) ^d	3.7	13.88	17.31 ^c	3.4
Cd($4d_{3/2}$)	11.46(9) ^e	3.9	15.36	18.28 ^c	2.9
Cd($4d_{5/2}$)	10.47(9) ^e	3.9	14.37	17.58 ^c	3.2
Pb($4f_{7/2}$)	136.4(2) ^d	4.05	140.5	144.0(5) ^f	3.5
Bi($4f_{7/2}$)	157.0(2) ^d	4.3	161.3	164.9(5) ^f	3.6

^aReference 20.^bReference 17.^cReference 15.^dThis work.^eReference 18.^fReference 19.

TABLE V. Binding energies from XPS in elemental solids and optimized HFS on atoms (in eV).

Level	E_B^F ^a	ϕ ^b	E_B^V	$E_B(\text{theo})$ ^c	ΔE_B
C 1s ^d	284.44(4)	4	288.4	297	8.6
Al 2s	118.4(2)	3.7	122.1	128	5.9
Al 2p	72.9(2)	3.7	76.6	80.7	4.1
Cu 2p _{1/2}	952.6(2)	4.5	957.1	959.7	2.6
Cu 2p _{3/2}	932.8(2)	4.5	937.3	939.3	2.0
Cu 3s	122.45(10)	4.5	126.95	132.0	5.05
Cu 3p _{1/2}	77.23(10)	4.5	81.7	85.5	3.8
Cu 3p _{3/2}	75.07(10)	4.5	79.6	82.9	3.3

^aFrom work in progress in this laboratory.^bReference 20.^cReference 16.^dGraphite form.

XPS binding energies E_B^V for core levels of a number of elements, accurate to ± 1 eV. Also given were optimized-HFS (OHFS) results for the atoms: orbital energies only in some cases and binding energies also in others. For those cases in which E_B (OHFS) was given direct comparisons can be made. In other cases rearrangement energies (from OHFS calculations) have now been given by Gelius and Siegbahn.²¹ Table VI lists, for several elements, E_B^V and E_B (atomic, OHFS), from Refs. 16 and 21, for the $n=2$ core levels. These were judged to give the most reliable comparisons. For 1s states the theory is less successful presumably because of quantum electrodynamic effects,¹¹ while the experimental values are also less accurate in an absolute sense because of high energies and wide lines. The $n=3$ data were excluded because multiplet splitting introduces uncertainties. Both the $n=1$ and the $n=3$ results are in general agreement with those in Table VI, however.

From Tables V and VI it is evident that ΔE_B is always positive. It varies considerably in magnitude, showing especially large values for graphite and for the heavy 3d transition-series metals, although it is small again for copper (Tables IV and V) and zinc (Tables II and IV).

C. Core-Level Binding Energies for Rare Gas Atoms Embedded in Metals

Siegbahn *et al.*¹⁶ gave binding energies for core levels of rare-gas atoms embedded in metal foils, as well as for free rare-gas atoms.²² The former were given as E_B^V . The free-atom binding energies were in most cases larger than those of the embedded atoms by $\sim 2-5$ eV. In Table VII the average differences $\langle \Delta E_B \rangle_{av}$ are listed for each of the four rare gases Ne, Ar, Kr, and Xe. Recently

TABLE VI. Additional XPS binding energies and optimized HFS results on atoms (in eV).

Level	$E_B(\text{theo})$ ^a	E_B^V ^b	ΔE_B
Na 2s	71.9	65	6.9
Na (2p)	36.6	33	3.6
Mg 2s	97.7	93	4.7
Mg (2p)	56.3	56	0.3
K 2s	386	379	7
K 2p _{1/2}	303	299	4
K 2p _{3/2}	300	296	4
Ca 2s	450.4	441	9.4
2p _{1/2}	360.9	353	7.9
2p _{3/2}	356.9	350	6.9
Sc 2s	511	504	7
2p _{1/2}	415	411	4
2p _{3/2}	410	406	4
Ti 2s	574	569	5
2p _{1/2}	473.6	465	8.6
2p _{3/2}	466.6	459	7.6
V 2s	641	632	9
2p _{1/2}	534	524	10
2p _{3/2}	525	517	8
Cr 2s	707.1	699	8.1
2p _{1/2}	593.6	588	5.6
2p _{3/2}	583.6	579	4.6
Mn 2s	785	773	12
2p _{1/2}	666	656	10
2p _{3/2}	653	645	8
Fe 2s	862.5	851	11.5
2p _{1/2}	735.8	728	7.8
2p _{3/2}	721.8	715	6.8
Co 2s	943	930	13
2p _{1/2}	810	798	12
2p _{3/2}	794	783	11
Ni 2s	1027.9	1013	14.9
2p _{1/2}	888.1	877	11.1
2p _{3/2}	869.1	860	9.1

^aFrom Ref. 16.^bFrom Refs. 16 and 20.

Citrin *et al.*²³ have repeated the measurements on rare-gas atoms embedded in metal foils. The differences ΔE_B between their results and the free-atom values²² are also set out in Table VII. We have also observed shifts of this kind for argon levels in connection with argon-ion bombardment procedures for cleaning metal surfaces. Our aver-

TABLE VII. Core-level binding-energy shifts for rare gases in metals (in eV).

Atom	$\Delta E_B(\text{Ref. 16})$ ^a	$\Delta E_B(\text{Ref. 23})$ ^b	$\Delta E_B(\text{this work})$ ^c
Ne	3.4	3.0	
Ar	3.6	2.6	2.8
Kr	3	2.5	
Xe	4	2.2	

^aAverage of several core levels.^bIn copper.^cAverage of 2p_{1/2}, 2p_{3/2}, and 3p shifts.

age result for the Ar $2p_{1/2}$, $2p_{3/2}$, and $3p$ levels is set out in Table VII. Again ΔE_B is always positive, ranging from 2.2 to 4 eV for these four rare gases.

The results of this section can be summarized as indicating that $\Delta E_B = E_B(\text{gas}) - E_B^V$ is always positive for atomic core levels, falling in a rather wide range of values up to ~ 15 eV. This shift cannot be assigned with certainty to any single effect, but we believe that extra-atomic relaxation is the dominant factor. This interpretation is supported by the rather good detailed agreement with experiment shown by an "extra-atomic relaxation" model derived in Sec. VI. There is, however, another effect that may also be important; namely, a change in the magnitude of the core level's orbital energy ϵ in the solid relative to that in the gas.²⁴ This change could apparently have either sign, depending on the details of the local bonding structure. It is difficult to estimate the magnitude of $\Delta\epsilon = \epsilon(\text{solid}) - \epsilon(\text{atoms})$, but we would expect it to be rather small for core levels, probably in the 1–2 eV range or less in most cases. It is difficult to see how $\Delta\epsilon$ would be substantially larger than this. If $\Delta\epsilon$ were very large for the $3d$ orbital in zinc, for example, very strong chemical bonds would have to be present. In fact the cohesive energy of zinc is less than 1 eV.

We can gain some insight into the relative importance of $\Delta\epsilon$ and the relaxation energy in molecules by comparing the orbital energies of the carbon- $1s$ electron in atomic carbon and in fluoromethanes. Two values that are available for $\epsilon(1s, \text{atomic carbon})$ are -308.5 ¹⁰ and -310 eV.¹⁶ In methane itself carbon is negatively charged and there is a *chemical* shift of $\epsilon(\text{C } 1s)$ down to -305.2 eV. There is, however, a good correlation between $\epsilon(1s)$ and gross atomic charge. The values of $\epsilon(\text{C } 1s)$ in CH_3F and CH_2F_2 have been found by Gelius *et al.*²⁵ to be -307.96 and -313.88 eV, respectively, while their gross carbon atomic charges are -0.13 and $+0.67$. Interpolation to zero charge gives $\epsilon \cong -308.9$ eV, or about the same as in atomic carbon. Thus $\Delta\epsilon \sim 1$ eV or less in this case, while the total relaxation energy is ~ 15 eV.²⁶

While ϵ does not change appreciably from atoms to molecules, provided that chemical shifts are excluded, and probably doesn't change very much from atoms to metals (with which we are concerned in this work), it seems likely that ϵ might change appreciably from an ion to an ionic solid. In that case the strongly attractive ionic forces could hold the solid together while $|\epsilon|$ for each ion core orbital was decreased relative to the free ion by the confining effect of being held in the lattice. This would increase the local electron density, make the core orbital environment more repulsive,

and decrease $|\epsilon|$. Even for ionic solids, however, this effect is strongly self-limiting. Binding-energy shifts from free atoms to solids appear on all core levels, and the same two-electron integrals that contribute to ϵ also contribute to the total energy. Thus that part of the negative shifts in E_B from atoms to solids that arises from $\Delta\epsilon$ will show up strongly in the total energy, raising it and making the solid unstable.

In summary, we believe that extra-atomic relaxation, rather than the $\Delta\epsilon$ effects, is dominant in the observed binding-energy shifts from atoms to metals. The $\Delta\epsilon$ effect, though probably small, is difficult to evaluate, and more work on it is clearly needed.

VI. SCREENING MODEL FOR SEMILOCALIZED EXCITONS

Extra-atomic relaxation in small molecules during core-state photoemission, by transfer of electronic charge through the chemical bonds, is well established.²⁶ Extra-atomic relaxation in solids has also been pointed out.¹³ From the discussion in Sec. V it now seems clear that extra-atomic relaxation is generally present during core-level photoemission from conducting solids. Indeed this should come as no surprise: It is simply a very direct experimental manifestation of "screening" of an excess charge—the hole—on an "impurity" by the itinerant electrons. Friedel suggested twenty years ago^{27,28} that screening of an impurity charge should be accomplished by the formation of an occupied semilocalized (exciton) state about the impurity via the dropping down of a conduction-band state below E_F at the impurity site. We assume that the outgoing photoelectron will interact repulsively with this nascent valence band state as the latter forms adiabatically during photoemission. This would be in complete analogy with atomic relaxation of the valence orbitals during photoemission from core states.¹³ Here, too, it would result in a lowering of the binding energy.

Hedin and Johansson²⁹ showed that the atomic binding energy E_B^i of an electron in an orbital $|i\rangle$ can be related to the orbital energy quite accurately by

$$E_B^i(\text{atomic}) = -\epsilon_i - \frac{1}{2} \langle i | V_p^a | i \rangle, \quad (5)$$

where V_p^a is an atomic "polarization potential" given by

$$V_p^a = V_a^* - V_a, \quad (6)$$

where V_a^* is the Hartree-Fock potential of the occupied passive orbitals in the (relaxed) final state of the atom and V_a is the Hartree-Fock potential in the initial ground state. Since we are interested in the case of an atom in a metal, the V_p term in a metal must include all passive orbitals that are

occupied in the final state, rather than just those atomic orbitals occupied in the initial state. Thus we can write formally

$$E_B^i(\text{metal}) = -\epsilon_i - \frac{1}{2} \langle i | V_p^a | i \rangle - \frac{1}{2} \langle i | V_p^{ea} | i \rangle, \quad (7)$$

where V_p^{ea} includes all orbitals newly occupied in the final state. The exciton state is the only new occupied orbital. There must also be a newly unoccupied orbital on balance, but it is relatively diffused through the lattice and thus interacts with the hole much less strongly than does the new semilocalized state. Thus only the latter need be considered in a first estimate of $\langle i | V_p^{ea} | i \rangle$.

Formally we can write the Coulomb interaction between the exciton state $|E\rangle$ and the hole state $|i\rangle$ as

$$\langle i | V_{ea}^* | i \rangle = J(iE) - \frac{1}{2} K(iE), \quad (8)$$

where J and K are Coulomb and exchange integrals, respectively, in standard Hartree-Fock notation. Now Friedel's theory gives us the quantitative Friedel sum rule

$$\delta = \frac{2}{\pi} \sum_L (2L+1) \eta_L, \quad (9)$$

which states that an impurity of charge δ relative to the lattice atoms will have its charge screened by net positive phase shifts in the conduction-electron partial- L waves. This does not indicate directly how to calculate J and K , because the wave function of the exciton state is not known. It is, however, expected that this state will be composed mainly of L waves corresponding to the symmetry of the lowest unbound states in the conduction band; e.g., the p wave in zinc, the d wave in iron, or the s (and p) wave in sodium. Furthermore, the wave function $|E\rangle$ of the exciton state, while oscillatory, will of course resemble an atomic wave function at the impurity ion core. We could therefore take

$$|E, \text{Zn}\rangle \sim |\text{Zn } 4p\rangle, \quad |E, \text{Fe}\rangle \sim |\text{Fe } 3d\rangle,$$

$$|E, \text{Na}\rangle \sim |\text{Na } 3s\rangle,$$

etc., for the purpose of roughly estimating $\langle i | V_p^{ea} | i \rangle$ for these metals.

Two more steps are necessary to facilitate a simple estimate of $\langle i | V_p^{ea} | i \rangle$: First we note that there is no exciton state before photoemission; thus

$$\langle i | V_p^{ea} | i \rangle = \langle i | V_{ea}^* | i \rangle. \quad (10)$$

Second, this hole-state integral would be tedious to calculate, since a Hartree-Fock hole-state calculation would first be necessary. It may, however, be quite accurately estimated using the "equivalent-cores" approximation¹³ in which an ion core with atomic number Z and a core hole is

replaced by an ion core of atomic number $Z+1$ and no hole; thus

$$\langle i, Z | V_p^{ea} | i, Z \rangle = \langle i, Z | V_E^* | i, Z \rangle \cong \langle i, Z+1 | V_E | i, Z+1 \rangle \quad (11)$$

and

$$|E, \text{Zn}\rangle \sim |\text{Ga } 4p\rangle, \quad |E, \text{Fe}\rangle \sim |\text{Co } 3d\rangle,$$

$$|E, \text{Na}\rangle \sim |\text{Mg } 3s\rangle. \quad (12)$$

With all these approximations we can now estimate for the $3d$ binding energy in zinc, for example,

$$E_B^Y(3d, \text{metallic Zn}) \cong E_B(3d, \text{atomic Zn}) - \frac{1}{2} [F^0(3d, 4p) - \frac{1}{15} G^1(3d, 4p) - \frac{3}{70} G^3(3d, 4p)]_{\text{gallium}}. \quad (13)$$

This gives $E_B^Y(3d, \text{metallic Zn}) \cong 17.3 - 4.8 = 12.5$ eV, in fairly good agreement with the experimental value $E_B^Y = 13.9$ eV. In fact this approach tends to *overestimate* ΔE_B , because the atomic $4p$ state on which it is based should be more localized than the exciton state.

Similar estimates of ΔE_B have been made for all of the elements considered in this paper. The equations that were used to estimate the extra-atomic relaxation energies for the ns core levels are

$$\frac{1}{2} \langle ns | V_p^{ea} | ns \rangle_Z \cong \frac{1}{2} [F^0(ns, ms) - \frac{1}{2} G^0(ns, ms)]_{Z+1}$$

or

$$\frac{1}{2} [F^0(ns, mp) - \frac{1}{6} G^1(ns, mp)]_{Z+1}$$

or

$$\frac{1}{2} [F^0(ns, md) - \frac{1}{10} G^2(ns, md)]_{Z+1}, \quad (14)$$

where the quantity chosen on the right-hand side depends on whether the exciton state is best approximated by an s , p , or d orbital. The coefficients of G^l were obtained from standard multiplet theory.³⁰ The corresponding equations for p orbitals are obtained in the same way. They are

$$\frac{1}{2} \langle np | V_p^{ea} | np \rangle_Z \cong \frac{1}{2} [F^0(np, ms) - \frac{1}{6} G^1(np, ms)]_{Z+1}$$

or

$$\frac{1}{2} [F^0(np, mp) - \frac{1}{6} G^0(np, mp) - \frac{1}{15} G^2(np, mp)]_{Z+1}$$

or

$$\frac{1}{2} [F^0(np, md) - \frac{1}{15} G^1(np, md) - \frac{3}{70} G^3(np, md)]_{Z+1}. \quad (15)$$

The only combinations that we actually used for d and f orbitals were

$$\frac{1}{2} \langle nd | V_p^{ea} | nd \rangle_Z \cong \frac{1}{2} [F^0(nd, ms) - \frac{1}{10} G^2(nd, ms)]_{Z+1}$$

or

$$\frac{1}{2} [F^0(nd, mp) - \frac{1}{15} G^1(nd, mp) - \frac{3}{70} G^3(nd, mp)]_{Z+1}$$

and

$$\frac{1}{2} \langle nf | V_p^{ea} | nf \rangle_z = \frac{1}{2} [F^0(nf, mp) - \frac{3}{70} G^2(nf, mp) - \frac{2}{83} G^4(nf, mp)]_{z+1}. \quad (16)$$

The results of these calculations are given and compared with experiment in Table VIII. For brevity only one value is given for each lattice, excepting copper and zinc, for which several accurate values are available. Average experimental values are also quoted for brevity. Thus for most of the 3*d* transition metals, for example, only the average value

$$\langle \Delta E_B \rangle_{av} = \frac{1}{2} [\Delta E_B(3s) + \Delta E_B(3p)] \quad (17)$$

is listed in Table VIII. Figure 4 is a plot of the experimental values of ΔE_B against values calculated on the above model. It shows that the two quantities are correlated. It also shows that $\Delta E_B(\text{theo}) > \Delta E_B(\text{expt})$ on the average, which is expected because this model is based on the highly localized atomic states: It must therefore over-estimate ΔE_B somewhat. The scatter of the

TABLE VIII. Experimental reduction in binding energies, and theoretical estimates based on atomic integrals for exciton states.

Element	Core level	Exciton state	$\Delta E_B(\text{theo})^a$	$\Delta E_B(\text{expt})$
C(graphite)	1s	2p	12.5	8.6 ^b
Ne (in Cu)	(c)	3s	4.0	3.0 ^d
Na	2s, 2p ^e	3s	5.0	5.3 ^e
Mg	2s, 2p	3p	4.9	2.5 ^e
Al	2s, 2p	3p	6.0	5.1 ^b
Ar (in Al)	(c)	4s	3.1	2.8 ^b
K	2s, 2p	4s	3.9	5.5 ^e
Ca	2s, 2p	3d	10.7	8.4 ^e
Sc	2s, 2p	3d	12.0	5.5 ^e
Ti	2s, 2p	3d	13.2	6.6 ^e
V	2s, 2p	3d	13.2	9 ^e
Cr	2s, 2p	3d	15.2	6.6 ^e
Mn	2s, 2p	3d	13.3	10.5 ^e
Fe	2s, 2p	3d	17.3	9.4 ^e
Co	2s, 2p	3d	18.3	12.3 ^e
Ni	2s, 2p	3d	18.4	12.5 ^e
Cu	b, c	4s, 4p	5.0	3.6 ^b
Cu	3d	4s, 4p	4.8	2.9 ^b
Zn	b, c	4p	5.0	5.2 ^b
Zn	3d	4p	4.8	3.4 ^b
Kr (in Cu)	(c)	5s	2.9	2.5 ^d
Cd	4d	5p	4.2	3.0 ^f
Xe (in Cu)	(c)	5s	2.5	2.2 ^d
Pb	4f _{7/2}	6p	5.2	3.5 ^g
Bi	4f _{7/2}	6p	5.6	3.6 ^g

^aCalculated from Mann's integrals (Ref. 10) using model discussed in text.

^bFrom work reported herein or in progress in this laboratory.

^cAverage of several core levels.

^dReference 23.

^eIn several cases the average shift for 2s and 2p electrons, from Table VI, was used for brevity. Data are from Ref. 16.

^fReference 18, and Table IV.

^gReference 19, and Table IV.

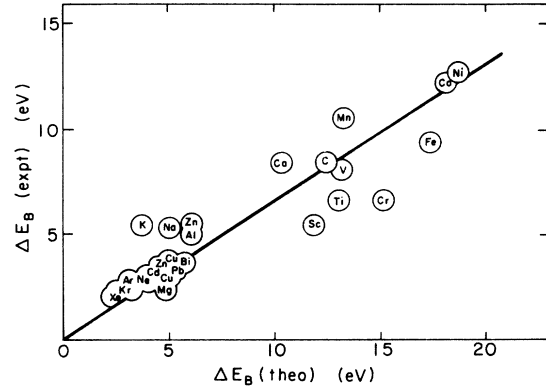


FIG. 4. Experimental excess binding energies in solids versus theoretical extra-atomic relaxation energies based on model described in text. Line through points has a slope of 0.66.

points in Fig. 4 could, we believe, arise largely from experimental error arising particularly from chemical shifts due to surface oxidation. Of course inadequacies in the model may also create scatter.

The correlation in Fig. 4 is encouraging, but more dramatic evidence for the validity of this model can be obtained by studying trends. In Fig. 5 experimental and theoretical shifts are plotted against atomic number for the 3*d* series and for

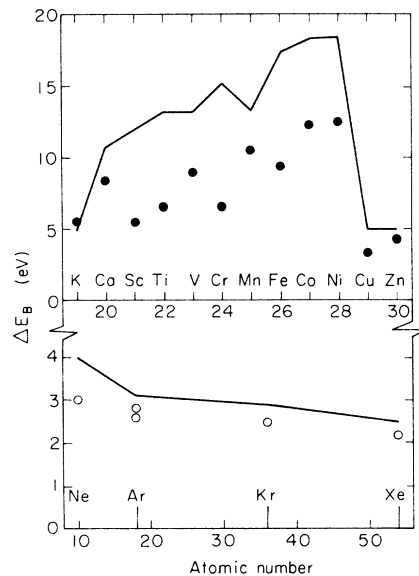


FIG. 5. Experimental excess binding energies (points) and theoretical estimates based on atomic-orbital approximation to exciton states, using model described in text (lines connecting calculated points). Top panel: results for 3*d* series metals. Note break at filled *d* shell, from Cu to Zn. Bottom panel: rare gases embedded in metals.

the rare-gas impurity series. The trends agree well in both series. Of special note is the sharp break in ΔE_B between Ni and Cu. This occurs because in Ni (atomic configuration $d^8 s^2$) there are d states immediately above E_F . The screening of a hole-state charge on the "impurity" is thus achieved mainly by the d wave. The exciton state is thus d like, and it interacts relatively strongly with the hole state [e.g., $F^0(2s, 3d)$ is large]. By contrast, in Cu (atomic configuration $3d^{10} 4s$) the d band is filled and screening must occur mostly via the s and p waves. The atomic approximation to the exciton state thus involves integrals such as $F^0(2s, 4s)$, which are smaller. It would be difficult to reproduce this dramatic break in ΔE_B at the top of the $3d$ series without explicitly considering atomic properties.

VII. CONCLUSIONS

Two major conclusions can be drawn from this work: First, relaxation effects are important in zinc, even for the $3d$ band. The question, "do the $3d$ bands lie below the bottom of the $4s, 4p$ bands?" is too simply stated. When its phraseology is refined, it has two answers. If one adds, "... in the photoemission spectrum?" the answer is "No, see Fig. 3." If one adds instead, "... in the initial state?" the answer is "Almost certainly yes, see Secs. IV and V." From Tables III and IV it seems evident that atomic relaxation of the $Zn(3d)$ orbitals amounts to about 4 eV and extra-atomic relaxation to about 3.4 eV. The binding energy $E_B(3d)$ is thus less than the orbital energy (Koopmans's theorem) estimates by 7.4 eV. Extra-atomic relaxation accompanying photoemission from the $4s, 4p$ bands is probably about

the same size or a little smaller [i.e., $F^0(4s, 4p) \cong F^0(3d, 4p)$] while atomic relaxation is smaller or even negative (Table III). Hence we would expect the $3d$ peak in the XPS spectrum to move ~ 5 eV closer to E_F relative to the $4s, 4p$ bands than their relative positions in a *self-consistent Hartree-Fock* calculation. Since most band-structure calculations are less rigorous than this, it is not clear where they "should" place the $3d$ bands in the initial state: probably higher. However the true d -band position would seem from this work to be at $\sim E_F - 15$ eV in the initial state. This result would thus be in rough agreement with the calculation by Mattheiss,⁷ which placed the $3d$ bands at ~ 17 eV below E_F . The large relaxation energy of the $3d$ bands in zinc carries implications for the photoemission spectrum of $3d$ transition-series metals. It seems possible that relaxation could distort the valence-band spectrum of nickel, for example. This might account for significant differences between the XPS spectrum and the density of states. Future interpretation of photoemission spectra should be made with relaxation in mind.

The second major conclusion from this work is that semilocalized exciton states accompanying photoemission have been identified through their effects on core-level binding energies in conductors. An approximate theoretical model was developed and used to estimate the extra-atomic relaxation energy accompanying the formation of these states. The model overestimates the effect somewhat, as expected, but it reproduces experimental trends very well. It appears to provide a first step toward a quantitative understanding of extra-atomic relaxation in metals.

*Work performed under the auspices of the U. S. Atomic Energy Commission.

[†]Present address: IBM, Thomas J. Watson Research Center, Yorktown Heights, N.Y. 10598.

¹A. E. Sandstrom, in *Handbuch der Physik*, edited by S. Flügge (Springer-Verlag, Berlin, 1957), Vol. XXX.

²C. Nordling, *Ark. Fys.* **15**, 397 (1959).

³P. O. Nilsson and I. Lindau, *J. Phys. F* **1**, 854 (1971).

⁴S. Hanzely and R. J. Liefeld, *Spec. Publ. Natl. Bur. Stand. (U. S.)* No. 323, 319 (1971).

⁵R. T. Poole, R. C. G. Leckey, J. G. Jenkin, and J. Liesegang (private communication).

⁶W. A. Harrison, *Phys. Rev.* **126**, 497 (1962).

⁷L. F. Mattheiss, *Phys. Rev.* **134**, A970 (1964).

⁸R. W. Stark and L. M. Falicov, *Phys. Rev. Lett.* **19**, 795 (1967).

⁹F. Borghese and P. Denti, *Nuovo Cimento B* **3**, 34 (1971).

¹⁰J. B. Mann, Report No. LA-3690, TID 4500 (unpublished).

¹¹A. Rosén and I. Lindgren, *Phys. Rev.* **176**, 114 (1968).

¹²C. C. Lu, T. A. Carlson, F. B. Malik, T. C. Tucker, and C. W. Nestor, *At. Data* **3**, 1 (1971).

¹³D. A. Shirley, *Chem. Phys. Lett.* **16**, 220 (1972).

¹⁴T. Koopmans, *Physica (Utr.)* **1**, 104 (1934).

¹⁵C. E. Moore, *Atomic Energy Levels*, Natl. Bur. Stds. Circ.

No. 467 (U. S. GPO, Washington, D. C., 1958), Vol. 3.

¹⁶K. Siegbahn, C. Nordling, A. Fahlman, R. Nordberg, K. Hamrin, J. Hedman, G. Johansson, T. Bergmark, S.-E. Karlsson, I. Lindgren, and B. J. Lindberg, *ESCA-Atomic, Molecular and Solid State Structure by Means of Electron Spectroscopy* (Nova Acta Regiae Soc. Sci. Upsaliensis, Upsala, Sweden, 1967), Ser. IV, Vol. 20.

¹⁷S. P. Kowalczyk, R. A. Pollak, F. R. McFeely, L. Ley, and D. A. Shirley, this issue, *Phys. Rev. B* **8**, 2387 (1973).

¹⁸R. A. Pollak, S. Kowalczyk, L. Ley, and D. A. Shirley, *Phys. Rev. Lett.* **29**, 274 (1972).

¹⁹Y. S. Khodeyev, H. Siegbahn, K. Hamrin, and K. Siegbahn, Report No. UUIP-802, 1972 (unpublished).

²⁰W. Gordy and W. J. O. Thomas, *J. Chem. Phys.* **24**, 439 (1956).

²¹U. Gelius and K. Siegbahn, Report No. UUIP-794, 1972 (unpublished).

²²K. Siegbahn, C. Nordling, G. Johansson, J. Hedman, P. F. Hedén, K. Hamrin, U. Gelius, T. Bergmark, L. O. Werme, R. Manne, and Y. Baer, *ESCA Applied to Free Molecules* (North-Holland, Amsterdam, 1969).

²³P. H. Citrin, D. R. Hamann, and S. Hüfner, *Bull. Am. Phys. Soc.* **1**, 55 (1973).

²⁴This effect was pointed out to us by R. E. Watson.

- ²⁵U. Gelius, P. F. Hedén, J. Hedman, B. J. Lindberg, R. Manne, R. Nordberg, C. Nordling, and K. Siegbahn, *Phys. Scr.* **2**, 70 (1970).
- ²⁶D. W. Davis and D. A. Shirley, *Chem. Phys. Lett.* **15**, 185 (1972).

- ²⁷J. Friedel, *Philos. Mag.* **43**, 153 (1952).
- ²⁸J. Friedel, *Adv. Phys.* **3**, 446 (1954).
- ²⁹L. Hedin and G. Johansson, *J. Phys. B* **2**, 1336 (1969).
- ³⁰J. C. Slater, *Quantum Theory of Atomic Structure* (McGraw-Hill, New York, 1960), Vol. 2, p. 287.